Clinical Kidney Journal

ckj

OXFORD

Leading European Nephrology

Clinical Kidney Journal, 2016, vol. 9, no. 3, 424–428

doi: 10.1093/ckj/sfw008
Advance Access Publication Date: 24 March 2016
Exceptional Case

EXCEPTIONAL CASE

A novel heterozygous mutation in the *ATP6V0A4* gene encoding the V-ATPase a4 subunit in an adult patient with incomplete distal renal tubular acidosis

Eri Imai[1], Shuzo Kaneko[1], Takayasu Mori[2], Tomokazu Okado[2], Shinichi Uchida[2] and Yusuke Tsukamoto[1]

[1]Department of Nephrology, Itabashi Chuo Medical Center, Tokyo, Japan and [2]Department of Nephrology, Graduate School of Medical and Dental Sciences, Tokyo Medical and Dental University, Tokyo, Japan

Correspondence to: Shuzo Kaneko; E-mail: shuzo-kaneko10@ob.md.tsukuba.ac.jp

Abstract

A 40-year-old Japanese man who had a medical history of hypokalemic periodic paralysis 4 months prior was hospitalized to undergo a cholecystectomy. Hypokalemia, nephrocalcinosis and alkaluria suggesting distal renal tubular acidosis (dRTA) were detected, but metabolic acidosis was not evident. An ammonium chloride/furosemide–fludrocortisone/bicarbonate loading test demonstrated a remarkable disability in urinary H^+ excretion. A novel heterozygous mutation in the *ATP6V0A4* gene encoding the vacuolar H^+-ATPase (V-ATPase) a4 subunit p.S544L was detected. Among cases of V-ATPase a4 mutations, this is the first case in which a heterozygous mutation developed to an incomplete or latent form of dRTA.

Key words: *ATP6V0A4*, distal renal tubular acidosis (dRTA), heterozygous mutation, V-ATPase a4 subunit

Introduction

Distal renal tubular acidosis (dRTA) is characterized by an inability to secrete H^+ in α-intercalated cells. The clinical manifestations of the disease consist of hyperchloremic metabolic acidosis, hypokalemia, hypercalciuria, hypocitraturia, urinary concentrating ability defect, recurrent urinary stone formation, nephrocalcinosis and bone demineralization. With regard to the genetic cause of dRTA, several currently known mutations have been identified in α-intercalated cells, including anion exchanger 1 (AE1), the B1 or a4 subunits of vacuolar H^+-ATPase (V-ATPase) and cytosolic carbonic anhydrase 2 (CA2) [1–3]. In cases of dRTA caused by V-ATPase mutations, the autosomal recessive form that manifests the disease in infancy is common [1].

We herein describe an adult patient with incomplete dRTA caused by a novel heterogeneous mutation of V-ATPase a4. Among cases of dRTA due to V-ATPase a4 mutations, this is the first case that developed to an incomplete or late-onset form of the disease.

Case report

A 40-year-old Japanese man was admitted to our hospital to undergo a laparoscopic cholecystectomy. An unknown hypokalemia [potassium (K) 2.7 mmol/L] was found and he was referred to our department presurgery. He had been hospitalized in another hospital for periodic paralysis due to unknown severe hypokalemia (K 1.7 mmol/L) 4 months prior. He and his father,

Received: November 28, 2015. **Accepted:** January 18, 2016

who had died of a stroke, had been diagnosed with nephrocalcinosis in their 20s. None of his three siblings had any medical history. His physical and laboratory findings were as follows: height, 182 cm; weight, 81.5 kg; blood pressure, 120/78 mmHg. No abnormalities were observed in a physical examination. His audibility test was normal. In a blood examination, his serum creatinine level was elevated at 1.44 mg/dL (127.3 μmol/L). His serum K level was low, at 2.7 mmol/L, while his sodium (Na), chlorine (Cl), calcium (Ca), phosphorus (P) and magnesium (Mg) levels were all normal, at 144 mmol/L, 108 mmol/L, 8.7 mg/dL, 2.7 mg/dL and 2.6 mg/dL, respectively. The venous bicarbonate (HCO_3^-) level was at the lower limit of the normal range, at 22.8 mmol/L. His blood anion gap was normal at 13.2. His complete blood counts were all normal. The levels of immunoglobulins and complements were all within normal limits, and he tested negative for antinuclear, anti-SS-A and anti-SS-B antibodies. The plasma renin activity (normal: 0.1–2) and plasma aldosterone concentration (normal: 35.7–240) were 0.7 ng/mL/h and 141.1 pg/mL, respectively. The spot urinary pH was 7.5 and the fractional excretion of K was inappropriately normal, at 10.3%, even in a hypokalemic state. The urinary Ca/creatinine ratio (mol) was 0.70. The urinary anion gap was positive at 30.9 (=Na 67 mmol/L + K 13.9 mmol/L – Cl [minus sign] 50 mmol/L). Abdominal CT revealed medullary nephrocalcinosis in both kidneys. A bone mineral density test showed normal levels. We suspected dRTA and started a prescription of potassium aspartate and sodium/potassium citrate during the perioperative period. The level of serum K was corrected to within the normal range at 3.6 mmol/L. Black-pigmented stones in the patient's gallbladder were detected after a successful laparoscopic cholecystectomy.

After suspension of the prescription for 7 days, the hypokalemia became advanced (K 3.0 mmol/L), while metabolic acidosis was not evident (HCO_3^- 29.3 mmol/L). We performed ammonium chloride (NH_4Cl), furosemide–fludrocortisone and HCO_3^- loading tests (Figures 1–3). The NH_4Cl loading test demonstrated that the patient had dysfunction in both urinary acidification and net acid excretion under the acid loading condition (Figure 1A–C). In the furosemide–fludrocortisone loading test, the potential to secrete H^+ into the lumina at distal nephrons with an enhanced negative charge was extremely weak (Figure 2A). In this test, instead of H^+, the patient's K secretion increased sharply compared with a healthy control (Figure 2B). In the bicarbonate loading test, the patient's basal H^+ secretion dysfunction was also demonstrated (Figure 3A); conversely, the tubular maximal reabsorption rate of HCO_3^- ($TmHCO_3^-$) was elevated compared with the control (Figure 3B).

We performed comprehensive genetic testing for known causal genes of RTA in the patient using next-generation sequencing (NGS) technology based on the capturing method (Agilent Technologies). The genes *SLC4A1* (encoding AE1), *ATP6V1B1*, *ATP6V0A1*, *ATP6V0A4* (encoding the B1, a1 and a4 subunits of V-ATPase, respectively), *SLC4A4* (encoding NBCe1-A), *SLC34A1* (encoding NaPi-2a) and *CA2* were all examined simultaneously. The detected mutations were narrowed down to those that might be disease-causing mutations according to the following two filters: one for novel variants that have not been reported

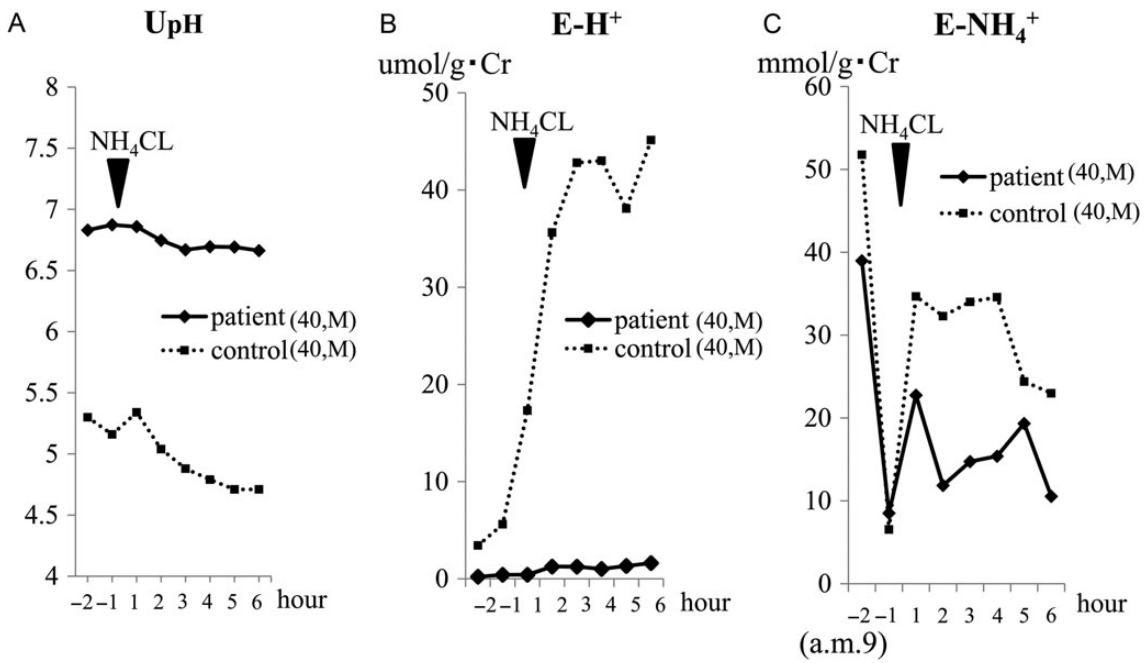

Fig. 1. Results of the NH_4Cl loading test. In the NH_4Cl loading test, 2 mg/kg per dose of NH_4Cl in powder form was orally administered to the patient. Urine samples were immediately sealed with liquid paraffin to minimize the ammonia gas loss and pH change. The urinary pH was immediately measured using a glass electrode pH meter and the urinary excretion of both H^+ (E-H^+) and NH_4^+ (E-NH_4^+) were defined as follows: E-H^+: urinary H^+/g · Cr; E-NH_4^+: urinary NH_4^+/g · Cr. Urinary H^+ and urinary NH_4^+ were calculated by the following formula: urinary H^+ (umol/L) = $10^3 \times 10^{-UPH}$, UpH = urinary pH; urinary NH_4^+ (uNH_4^+) (mmol/L) = (measured-Uosm (osm/L) – uGlu/18 – uUN/2.8)/2 – (uNa+ uK), uGlu = urinary glucose (mg/dL), uUN = urinary urea nitrogen (mg/dL), uNa = urinary Na (mmol/L), uK = urinary K (mmol/L). The tests were also performed on an age- and sex-matched healthy volunteer as a control in the same way. (**A**) The patient's UpH was much higher than that of the control. After loading, in contrast to that of the control, urinary acidification was not evident in the patient. (**B**) To correct any influences derived from a difference in the urinary dilution/concentration between the two, E-H^+, which denotes the relative amount of isolated H^+, was calculated. The differences in the E-H^+ level and in its change after loading were more prominent than those for UpH. The ratio of the patient's E-H^+ to that of the control during the test was in the range of 0.023–0.062. (**C**) E-NH_4^+ mainly reflects the net acid excretion in the urine. The patient's E-NH_4^+ was smaller to that of the control. The ratio of the patient's E-NH_4^+ to that of the control during the test was in the range of 0.37–0.67. Note that the patient/control ratio of E-NH_4^+ was more than 10 times larger than that of E-H^+.

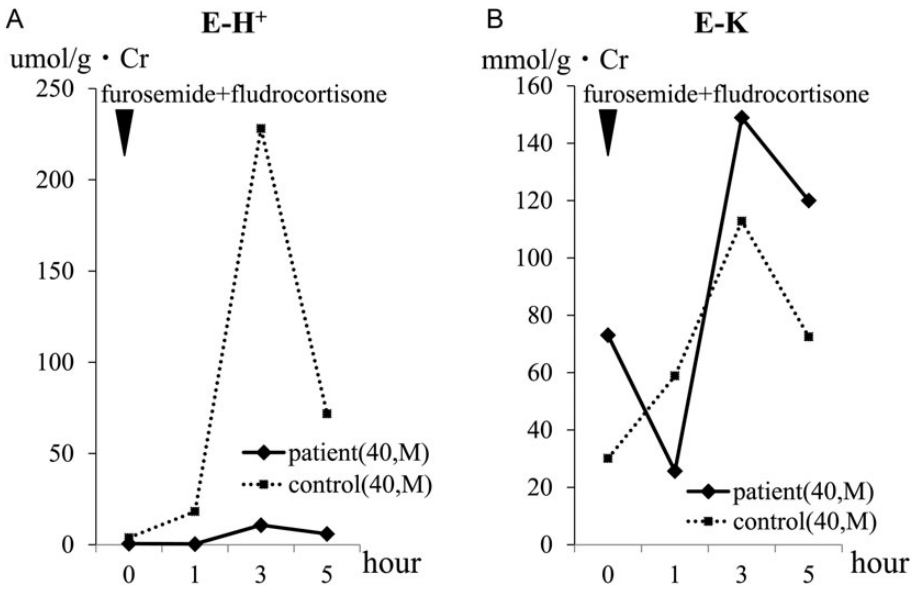

Fig. 2. Results of the furosemide–fludrocortisone loading test. In the furosemide–fludrocortisone loading test, 40 mg of furosemide and 1 mg of fludrocortisone per dose were orally administered to the patient. UpH was immediately measured using a glass electrode pH meter and E-H^+ and E-K (defined as urinary K/g·Cr) were calculated. (**A**) In both the patient and the control, the level of E-H^+ reached its peak at 3 h after loading and then decreased. The level of the patient's E-H^+ during the test was extremely low compared with that of the control. (**B**) The patient's E-K transiently decreased at 1 h after loading, but then increased sharply compared with that of the control. Both the maximum and final level of the patient's E-K during the test were higher than that of the control.

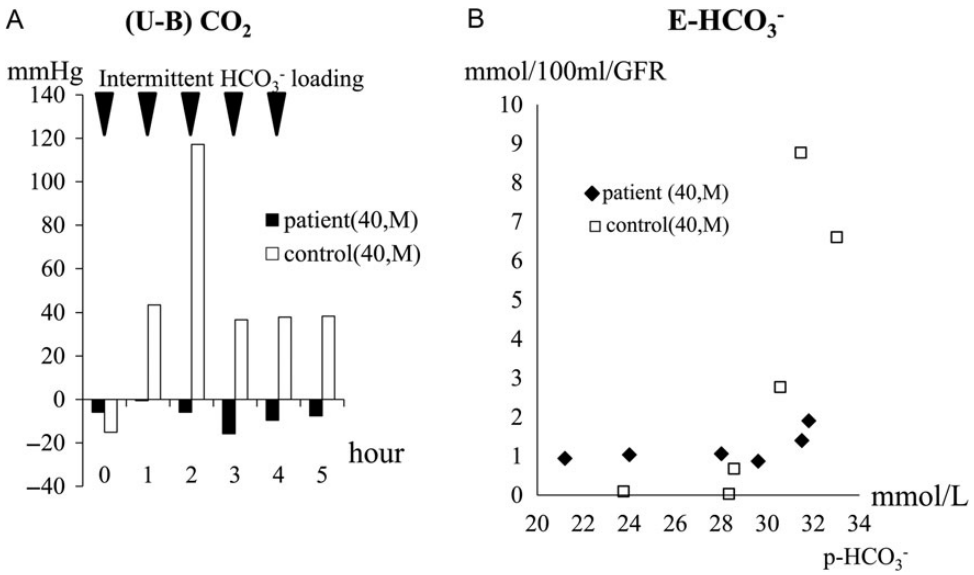

Fig. 3. Results of the HCO_3^- loading test. In the HCO_3^- loading test, 0.08 g/kg per dose of HCO_3^- in powder form was orally administered to the patient five times hourly during the test. Urine samples were immediately sealed with liquid paraffin to minimize the carbon dioxide (CO_2) gas loss and pH change. All blood and urine samples was immediately measured using a gas analyzer or a glass electrode pH meter. (U-B) CO_2 and net excretion HCO_3^- (E-HCO_3^-) were calculated by the following formula: (U-B) CO_2 (mmHg) = $uCO_2 - bCO_2$ [uCO_2 = urinary CO_2 (mmHg), bCO_2 = blood CO_2 (mmHg)]; E-HCO_3^- (mmol/100 mL/GFR) = $0.1 \times (uHCO_3^- + uCO_2 \times 0.0301) \times sCr/uCr$ (GFR = glomerular filtration rate); uHCO_3^- (urinary HCO_3^-) (mmol/L) = $0.0301 \times uCO_2 \times 10^{UpH-UPK'}$, $UPK' = 6.33–0.5 \times \sqrt{(uNa/1000 + uK/1000 + uNH_4^+/1000)}$ [sCr = serum creatinine (mg/dL), uCr = urinary creatinine (mg/dL)]. (**A**) (U-B) CO_2 denotes the states of basal H^+ secretion in distal nephrons. In the control, an increase of the (U-B) CO_2 level, which indicates a basal state of H^+ secretion accompanied by a dose-dependent accumulation of HCO_3^- filtrate overflowing into the lumens of distal nephrons, was observed in the first half period of the test, while the levels of (U-B) CO_2 were kept down, which was assumed to be an 'adaptive change' (i.e. suppression of H^+ secretion) against advanced metabolic alkalosis in the second half period. In the patient, however, (U-B) CO_2 remained almost unchanged at extremely low levels during the test. (**B**) The level of E-HCO_3^- rose abruptly when the plasma HCO_3^- (p-HCO_3^-) level exceeded $TmHCO_3^-$. In the test, the level of the patient's $TmHCO_3^-$ was relatively high, at approximately 32 mmol/L, compared with that of the control (28 mmol/L). Under a level of p-HCO_3^- lower than that of $TmHCO_3^-$, the patient's E-HCO_3^- was slightly detected (at approximately 1 mEq/min/GFR) while that of the control was not detected at all. The reason for this is explained by the difference in the acid/alkaline state of the urine samples between the two subjects. In an acid state, HCO_3^- is easily converted to CO_2 gas and lost from the samples, while this does not occur in an alkaline state.

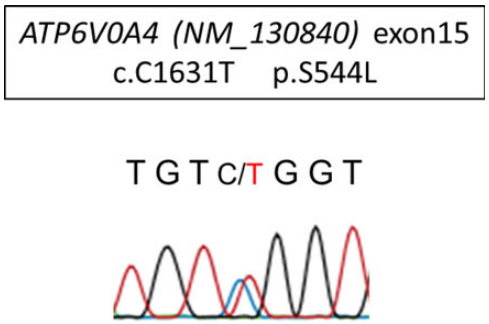

Fig. 4. Results of Sanger sequencing of the identified mutation in *ATP6V0A4*. The mutation C1631T located on exon15 was consistent with that of multiplex genetic testing.

previously or for variants with minor allele frequencies (MAFs) of up to 1% in the four single nucleotide polymorphism (SNP) databases [Human Genetic Variation Database (Japanese) [4], 1000 Genomes [5], ESP6500 [6], Exome Aggregation Consortium [7]] and a second one for variants except for synonymous mutations if the variants are in the coding region. Consequently, only one mutation, which is a novel heterozygous mutation in *ATP6V0A4* (exon 15, c.C1631T, p.S544L) was detected. As shown in Figure 4, the detected variants were validated with conventional Sanger sequencing and the result was consistent with that of the NGS diagnosis. Moreover, to confirm whether a large structural variant such as a large deletion or insertion exists as the second mutation, we performed the copy number variation (CNV) analysis for all the targeted genes by using CONTRA (Supplementary Ref S1). Briefly, this is CNV detection software using NGS data, and it calls copy number gains and losses for each target region by comparing the normalized sequencing depth from control samples. We used the sequence data from seven individuals as controls and did not find any large deletions or insertions in the patient. The results of CNV detection extracting the *ATP6V0A4* region are shown in Supplementary Table S1. There were no regions where relative sequencing depth was significantly changed compared with the controls, indicating that this patient did not have large deletions in *ATP6V0A4*, thus he was believed to be a heterozygous carrier of the *ATP6V0A4* mutation. In addition, it was confirmed at the same time that other tested genes (*SLC4A1*, *SLC4A4*, *ATPV1B1*, *ATPV0A1*, etc.) did not have any CNVs.

Discussion

As for the genetic causes of dRTA, the culprit protein can be detected in AE1, V-ATPase or CA2, expressed in α-intercalated cells. The late-onset or incomplete/mild type of dRTA is common in autosomal dominant, heterozygous mutations of AE1 [1–3]. The clinical manifestation in the present case resembled cases caused by heterozygous AE1 mutations responsible for the following attributes: late onset, subclinical metabolic acidosis and complicated gallbladder stones. In dRTA from mutant AE1, an aberrant AE1 expressed on the cell membranes of erythrocytes can be a cause of hemolysis and gallbladder stones [1]; however, the relationship between dRTA and gallbladder stones in the present case remains unclear because neither hemolysis nor AE1 mutations were evident.

In cases of dRTA caused by mutant V-ATPase in either the B1 or a4 subunit, >40 gene mutations encoding each of those subunits have been reported to date [8–12]. The B1 subunit consists of a cytoplasmic V1 domain that hydrolyzes ATP, while the a4 transmembrane V0 domain translocates H^+ [13]. Cases of dRTA caused by mutant B1 have been recognized to develop deafness early in the disease course, while those caused by mutant a4 do not develop deafness or exhibit deafness with a highly variable phenotype range [13–16]. In relation to the critical form of dRTA, hardly any difference between B1 and a4 in clinical manifestation was observed. However, according to a report from Turkey, polyuria and nephrocalcinosis were more common in dRTA patients with deafness compared with patients without deafness. This may suggest the difference between B1 and a4 in dRTA [17]. The difference in both the distribution and roles played by these two subunits may influence the clinical manifestation; however, the information derived from long-term observation was inconclusive.

In the critical form of mutant V-ATPase, the autosomal recessive form, showing an early onset (developing in infancy) and severe metabolic acidosis, was common until quite recently. However, incomplete dRTA presenting as impaired urinary acidification and/or recurrent renal stones from a heterozygous mutation or polymorphism of the B1 subunit has been reported [18, 19]. Zhang *et al.* [18] investigated a family of dRTA patients with a B1 subunit gene mutation (p.F468fsX487) and demonstrated impairment of urinary acid acidification and net acid excretion in heterozygotes with normal plasma HCO_3^-. They also showed an aberrant distribution and expression of mutant B1 in the renal papilla of a heterozygote with severe kidney stones, and demonstrated insufficient V-ATPase activity of the heterologous expression of wild and mutant B1 using transfected mammalian cells and yeast. Most recently, Dhayat *et al.* [19] investigated a total of 555 recurrent stone formers and showed that the impairment of urinary acidification in acute NH_4Cl loading, suggesting incomplete dRTA, was significantly observed in a population that was a heterozygous for the p.E161K SNP in subunit B1. In the present case, there was no variant in *ATP6V1B1* (c.481G, p.161E). In regard to the a4 subunit of V-ATPase, to the best of our knowledge, the clinical features of a heterozygous a4 mutant in humans have not been well described to date, but in wild/*ATP6V0a4*-deletion hybrid mice, hyperchloremic metabolic acidosis under the condition of chronic acid loading has been proven [20]. It is clinically important that the incomplete dRTA from a novel heterozygous V-ATPase a4 subunit mutation in the present case presents as severe hypokalemia and chronic renal insufficiency. None of the six heterozygotes in a mutant B1 subunit described in a recent report [18] had this clinical feature. The loading tests for the present case clearly explained the mechanism of the clinical features, namely a urinary H^+ excretion dysfunction with compensatory changes in the proximal tubules (i.e. enhanced NH_4^+ production, $TmHCO_3^-$ elevation) and urinary K loss instead of H^+. No examinations of the patient's siblings have been done, but these changes may not be specific to the mutation of the present case, as the common mechanisms may be at work in any type of incomplete dRTA caused by a heterozygous mutant V-ATPase.

In terms of the NGS analysis, especially in CNV, it has been well known that detecting relatively large structural variants is still a developing issue in NGS analysis. Moreover, particularly in cases of targeted resequencing like this one, it becomes more difficult to detect CNVs since the sequenced regions are very limited compared with the whole genome (Supplementary Ref S2) and thus detection sensitivity may decrease. Therefore, even though the CNV detection approach was done for NGS data, there remains the possibility that we could not detect such variants perfectly. This could be one of the limitations of this genetic analysis.

Clinical Kidney Journal
ckj

Supplementary data

Supplementary data are available online at http://ndt.oxfordjournals.org.

Conflict of interest statement

None declared.

References

1. Batlle D, Haque SK. Genetic causes and mechanisms of distal renal tubular acidosis. *Nephrol Dial Transplant* 2012; 27: 3691–3704
2. Rodríguez Soriano J. Renal tubular acidosis: the clinical entity. *J Am Soc Nephrol* 2002; 13: 2160–2170
3. Both T, Zietse R, Hoorn EJ *et al*. Everything you need to know about distal renal tubular acidosis in autoimmune disease. *Rheumatol Int* 2014; 34: 1037–1045
4. Narahara M, Higasa K, Nakamura S *et al*. Large-scale East-Asian eQTL mapping reveals novel candidate genes for LD mapping and the genomic landscape of transcriptional effects of sequence variants. *PLoS One* 2014; 9: e100924
5. 1000 Genomes Project Consortium. A map of human genome variation from population-scale sequencing. *Nature* 2010; 467: 1061–1073
6. Exome Variant Server, NHLBI GO Exome Sequencing Project, Seattle, WA. http://evs.gs.washington.edu/EVS/ (December 2014, date last accessed).
7. Exome Aggregation Consortium (ExAC), Cambridge, MA. http://exac.broadinstitute.org (July 2015, date last accessed)
8. Miura K, Sekine T, Takahashi K *et al*. Mutational analyses of the *ATP6V1B1* and *ATP6V0A4* genes in patients with primary distal renal tubular acidosis. *Nephrol Dial Transplant* 2013; 28: 2123–2130
9. Elhayek D, Perez de Nanclares G, Chouchane S *et al*. Molecular diagnosis of distal renal tubular acidosis in Tunisian patients: proposed algorithm for Northern Africa populations for the *ATP6V1B1*, *ATP6V0A4* and *SCL4A1* genes. *BMC Med Genet* 2013; 14: 119
10. Nagara M, Voskarides K, Nouira S *et al*. Molecular investigation of distal renal tubular acidosis in Tunisia, evidence for founder mutations. *Genet Test Mol Biomarkers* 2014; 18: 741–748
11. Pereira PC, Melo FM, De Marco LA *et al*. Whole-exome sequencing as a diagnostic tool for distal renal tubular acidosis. *J Pediatr (Rio J)* 2015; 91:583–589
12. Gómez J, Gil-Peña H, Santos F *et al*. Primary distal renal tubular acidosis: novel findings in patients studied by next generation sequencing. *Pediatr Res* 2015; doi:10.1038/pr.2015.243
13. Breton S, Brown D. Regulation of luminal acidification by the V-ATPase. *Physiology (Bethesda)* 2013; 28: 318–329
14. Stover EH, Borthwick KJ, Bavalia C *et al*. Novel *ATP6V1B1* and *ATP6V0A4* mutations in autosomal recessive distal renal tubular acidosis with new evidence for hearing loss. *J Med Genet* 2002; 39: 796–803
15. Li X, Chai Y, Tao Z *et al*. Novel mutations in ATP6V0A4 are associated with atypical progressive sensorineural hearing loss in a Chinese patient with distal renal tubular acidosis. *Int J Pediatr Otorhinolaryngol* 2012; 76: 152–154
16. Gao Y, Xu Y, Li Q *et al*. Mutation analysis and audiologic assessment in six Chinese children with primary distal renal tubular acidosis. *Ren Fail* 2014; 36: 1226–1232
17. Topaloglu R, Baskın E, Bahat E *et al*. Hereditary renal tubular disorders in Turkey: demographic, clinical, and laboratory features. *Clin Exp Nephrol* 2011; 15: 108–113
18. Zhang J, Fuster DG, Cameron MA *et al*. Incomplete distal renal tubular acidosis from a heterozygous mutation of the V-ATPase B1 subunit. *Am J Physiol Renal Physiol* 2014; 307: F1063–F1071
19. Dhayat NA, Schaller A, Albano G *et al*. The vacuolar H^+-ATPase B1 subunit polymorphism p.E161K associates with impaired urinary acidification in recurrent stone formers. *J Am Soc Nephrol* 2015 ; doi:10.1681/ASN.2015040367
20. Norgett EE, Golder ZJ, Lorente-Cánovas B *et al*. *Atp6v0a4* knockout mouse is a model of distal renal tubular acidosis with hearing loss, with additional extrarenal phenotype. *Proc Natl Acad Sci USA* 2012; 109: 13775–13780